Nuclear Inst. and Methods in Physics Research, A 877 (2018) 51–55

Contents lists available at ScienceDirect

Nuclear Inst. and Methods in Physics Research, A

journal homepage: www.elsevier.com/locate/nima

Measurements of the reverse current of highly irradiated silicon sensors to determine the effective energy and current related damage rate

Moritz Wiehe *, S. Wonsak, S. Kuehn, U. Parzefall, G. Casse

Albert-Ludwigs-Universität Freiburg, Physikalisches Institut, Hermann-Herder-Str. 3, 79104 Freiburg, Germany
University of Liverpool, Oliver Lodge Building, Department of Physics, Oxford Street, L68 7ZE Liverpool, United Kingdom
CERN, Route du Meyrin 285, CH-1211 Genève 23, Switzerland

ARTICLE INFO

Keywords:
Silicon sensors
High irradiation environment
Reverse current measurement
Current related damage rate
Effective energy

ABSTRACT

The reverse current of irradiated silicon sensors leads to self heating of the sensor and degrades the signal to noise ratio of a detector. Precise knowledge of the expected reverse current during detector operation is crucial for planning and running experiments in High Energy Physics. The dependence of the reverse current on sensor temperature and irradiation fluence is parametrized by the effective energy and the current related damage rate, respectively. In this study 18 n-in-p mini silicon strip sensors from companies Hamamatsu Photonics and Micron Semiconductor Ltd. were deployed. Measurements of the reverse current for different bias voltages were performed at temperatures of −32 °C, −27 °C and −23 °C. The sensors were irradiated with reactor neutrons in Ljubljana to fluences ranging from 2×10^{14} n_{eq}/cm^2 to 2×10^{16} n_{eq}/cm^2. The measurements were performed directly after irradiation and after 10 and 30 days of room temperature annealing. The aim of the study presented in this paper is to investigate the reverse current of silicon sensors for high fluences of up to 2×10^{16} n_{eq}/cm^2 and compare the measurements to the parametrization models.

1. Introduction

Silicon sensors are widely used in High Energy Physics. In modern experiments like CMS and ATLAS, with high luminosity and particle energy, the sensors as well as electronic readout devices have to withstand a very harsh radiation environment. To study the radiation damage occurring during operation, detector components are irradiated to fluences of up to 2×10^{16} n_{eq}/cm^2.

For the operation of silicon sensors and the design of related detector components, e.g. the cooling system, one has to be able to predict the reverse current of the sensor. Among other parameters like the sensor volume, the reverse current strongly depends on the sensor temperature and the fluence Φ. For the parametrization of the temperature dependence the effective energy E_{eff} is commonly used as a scaling parameter [1]. Furthermore experimentally a linear relationship between irradiation fluence and reverse current was found, which is described by the current related damage rate α [2–5].

This study is related to previous measurements performed by Sven Wonsak [6]. It was observed, that the effective energy E_{eff} decreases for sensors irradiated with fluences higher than 1×10^{15} n_{eq}/cm^2. The aim of the study presented in this paper is to investigate the reverse current of silicon sensors, irradiated with reactor neutrons in Ljubljana to fluences of up to 2×10^{16} n_{eq}/cm^2, and determine if the parametrization models hold at high fluences expected in High Luminosity LHC (HL-LHC) operation (as given in e.g. Ref. [7]).

2. Models

2.1. Effective energy E_{eff}

The ratio of reverse currents $I(T)$ at two different temperatures T_1 and T_2 is described by Eq. (1), where k_B denotes the Boltzmann constant. With this relation it is possible to determine the effective energy E_{eff} by measuring the reverse current at different temperatures. Also for a known effective energy it allows to predict the reverse current at a certain temperature, given the reverse current at some reference temperature.

For silicon sensors the literature states a value of the effective energy of $E_{eff} = (1.214 \pm 0.014)$ eV [1].

$$\frac{I(T_2)}{I(T_1)} = \left(\frac{T_2}{T_1}\right)^2 \exp\left(\frac{-E_{eff}}{2k_B}\left[\frac{1}{T_2} - \frac{1}{T_1}\right]\right) \quad (1)$$

* Corresponding author at: Albert-Ludwigs-Universität Freiburg, Physikalisches Institut, Hermann-Herder-Str. 3, 79104 Freiburg, Germany.
E-mail address: moritz.wiehe@cern.ch (M. Wiehe).

http://dx.doi.org/10.1016/j.nima.2017.09.021
Received 28 June 2017; Received in revised form 7 September 2017; Accepted 10 September 2017
Available online 25 September 2017
0168-9002/

2.2. Current related damage rate

Experimentally one observes a linear dependence of the increase of the reverse current due to irradiation on the irradiation fluence, corresponding to Eq. (2). $I(\Phi_0)$ and $I(\Phi_{eq})$ are the reverse currents before and after irradiation with fluence Φ_{eq}. The constant of proportionality α is called current related damage rate.

$$I(\Phi_{eq}) - I(\Phi_0) = \Delta I = \alpha \cdot \Phi_{eq} V \tag{2}$$

Usually the depleted detector volume (V) has to be known to calculate the current related damage rate. The sensors irradiated to very high fluences, as presented in this study, cannot be fully depleted. Furthermore TCT-measurements have shown that the theoretically neutral area in a not fully depleted sensor is not completely free of an electric field [1,8]. Therefore the *geometric current related damage rate* α^* is used instead, using the full physical volume for calculation. This procedure is described in Ref. [6]. For a fully depleted sensor α and α^* are the same.

3. Experimental method

3.1. Sensors

For the measurements of the reverse current 18 n-in-p mini strip sensors from Hamamatsu Photonics K.K. [9] and Micron Semiconductor Ltd. [10] were used. The Hamamatsu sensors have a thickness of 293 μm and an active area of (0.8348×0.86) cm^2. The sensors from Micron are 143 and 50 μm thick and have an active area of (1.0985×1.0973) cm^2. The sensors were irradiated to fluences from 2×10^{14} to 2×10^{16} n_{eq}/cm^2 with reactor neutrons in Ljubljana.

3.2. Experimental setup

The goal was to measure the reverse current and sensor temperature while varying the bias voltage (IV-measurement). The measurements had to be performed at different sensor temperatures well below the freezing point while it was important to keep the sensor temperature as constant as possible during each measurement. Similar setups were developed in Liverpool and Freiburg. The sensors were glued on a Printed Circuit Board (PCB) for connection of the bias voltage. A PT1000 temperature sensor was glued directly onto the silicon sensor to measure the temperature as precise as possible. A photo of the test setup and one sensor is shown in Fig. 1. The PCB is mounted onto an aluminum-jig, which is cooled primarily with a Peltier-element. The cooling-rate is controlled with a PID-controller, for which the sensor temperature measured by the PT1000 is used as input. To remove the heat from the warm side of the Peltier-element the whole structure is connected to a metal block. A chiller allows to cool the block down. For the prevention of ice at temperatures below the freezing point a Perspex cover (not shown in picture) is placed on top of the Peltier system to create a box which is flushed with nitrogen.

In Liverpool, Nylon screws and heat conducting paste are used to connect the different parts of the active cooling system (aluminum-jig, Peltier-element and cold block) whereas in Freiburg these parts are glued together directly and in addition the whole setup is placed inside a commercial freezer to sustain a stable environment temperature. For voltage supply and current measurement a Keithley 237 voltage source is used.

3.3. Measurements

Measurements of the reverse current were performed at temperatures of −32 ° C, −27 ° C and −23 ° C directly after irradiation and after 10 and 30 days of room temperature annealing.

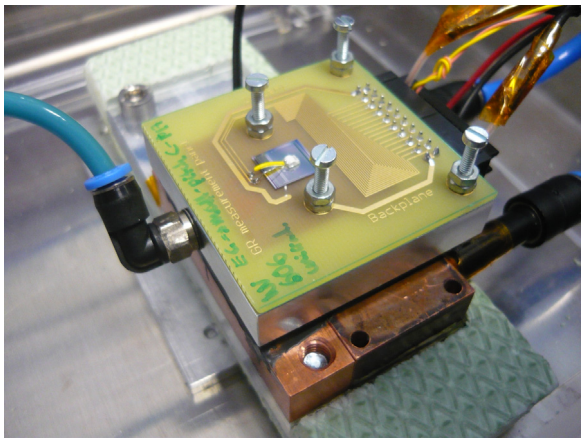

Fig. 1. Photo of the test setup: silicon sensor glued on PCB; temperature read-out with a PT1000, glued on top of the sensor.

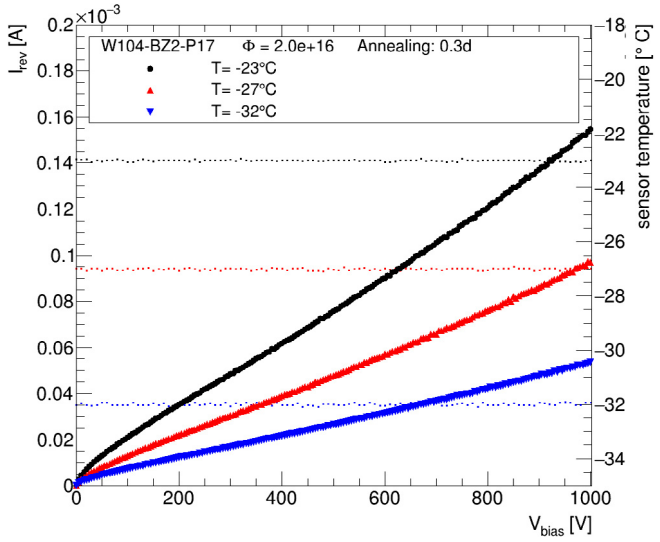

Fig. 2. Reverse current of sensor HPK W104-BZ2-P17 at three different temperatures. The horizontal, dotted lines show every second temperature measurement.

In the preceding study [6] during measurements at higher voltages a severe self-heating of the sensors was observed. The measured temperature varied by several Kelvin during a voltage scan from 0 to 1000 V. To minimize this effect for measurements presented here, special care was taken to stabilize the temperature of the sensor. During the measurements presented here, no self-heating of the sensor was observed. In Fig. 2 IV-measurements of an irradiated ($\Phi = 2 \times 10^{16}$ n_{eq}/cm^2) Hamamatsu sensor are shown as an example. Even for the highest fluence the temperature was kept constant during a complete voltage scan. Also it can be noted that from the IV-curve at this fluence it is not possible to tell when, if at all, the full depletion voltage is reached. Measurements of the reverse current at a temperature of −32 ° C and a bias voltage of 500 V are shown in Fig. 3 for all sensors. The values were scaled to ambient temperature.

4. Analysis method

4.1. Effective energy

To determine the effective energy for each sensor IV-measurements at three different temperatures (−32 ° C, −27 ° C, −23 ° C) were used.

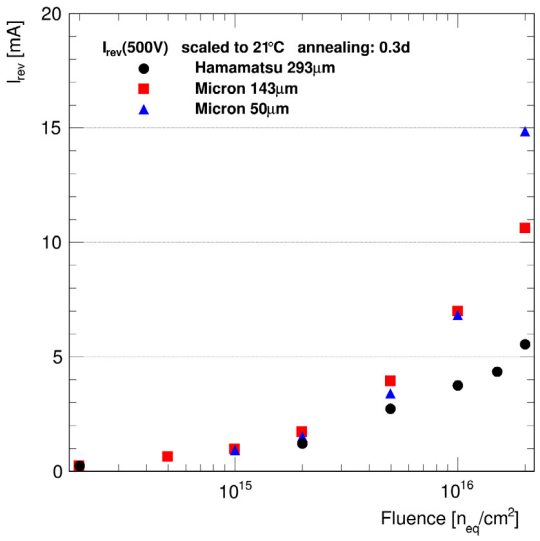

Fig. 3. Reverse current of all sensors measured after irradiation at a bias voltage of 500 V at −32 ° C. The measurements were scaled to ambient temperature.

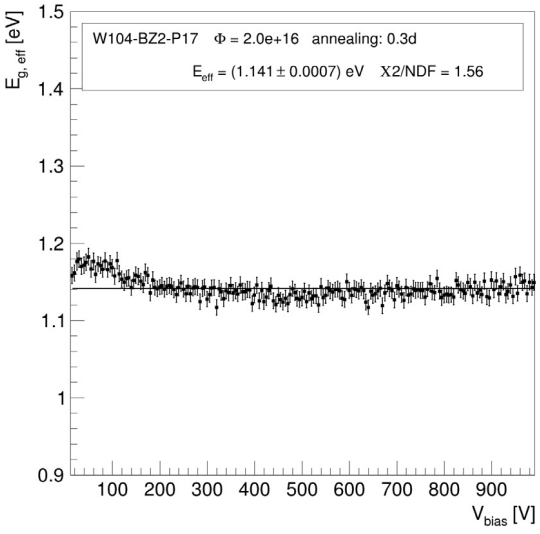

Fig. 4. Dependency of the effective energy on bias voltage for a 293 μm Hamamatsu sensor measured directly after irradiation to $\Phi = 2 \times 10^{16}$ n_{eq}/cm^2.

The data was fitted with the function

$$I(T) = A \cdot T^2 \, e^{-\frac{E_{eff}}{2k_B T}}, \tag{3}$$

where I is the reverse current measured at temperature T. A and E_{eff} are free fit parameters, with the latter being the effective energy; k_B denotes the Boltzmann constant. The measurements were performed at different voltages, which is not expected to influence the resulting value for the effective energy. Although for some sensors a dependency on bias voltage was observed. The values were averaged over the full voltage range, with the voltage dependency being accounted for by a systematic uncertainty of 0.03 eV on the final result.

4.2. Current related damage rate

For a calculation of the geometric current related damage rate α^*, according to Eq. (2), the IV-measurements of the irradiated sensors at $T = -32$ ° C are used and scaled to a temperature of $T = 21$ ° C, by using Eq. (1). The effective energy used for the scaling of the measured values was set to the literature value of $E_{eff} = 1.214$ eV for all measurements, to not distort the annealing behavior by variations of the scaling parameter. The physical detector volume was used rather

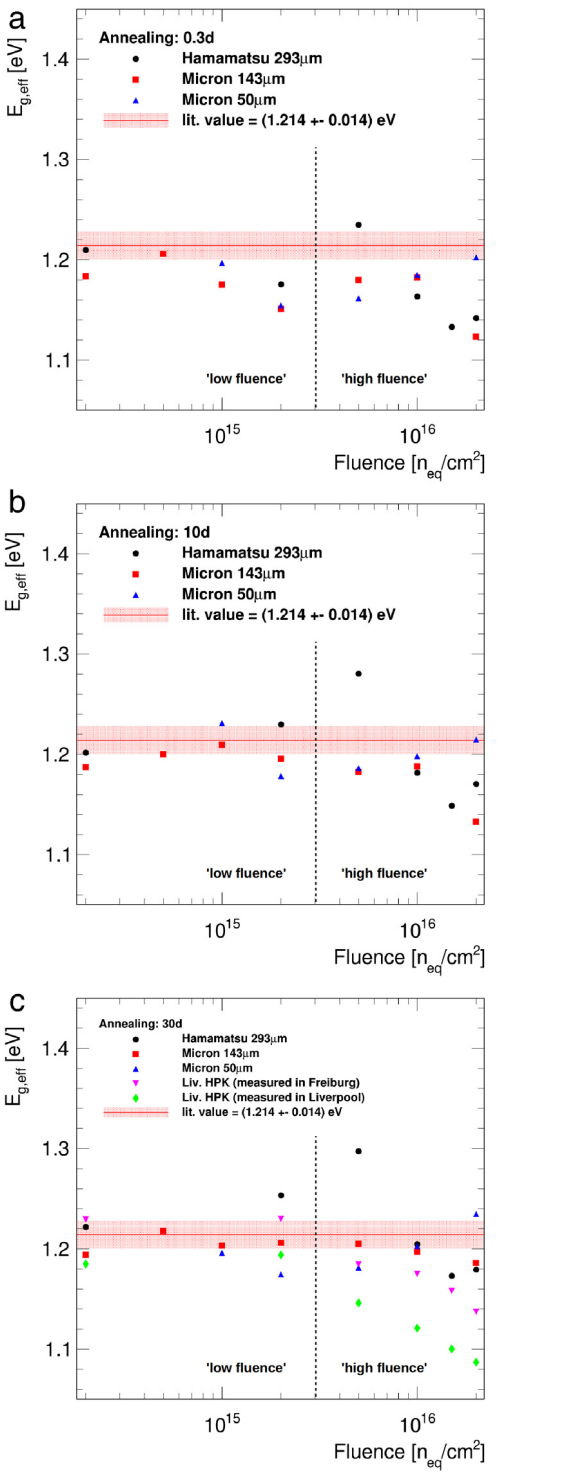

Fig. 5. Effective energy for different particle fluences measured directly after irradiation (a) and after 10 (b) and 30 (c) days annealing at room temperature. For the sake of clarity, error bars are not shown. The overall error is dominated by a systematic uncertainty of 0.03 eV, due to the voltage dependence of the effective energy. The last figure additionally includes measurements performed in Liverpool. The literature value of $E_{eff} = 1.214$ eV is shown as a horizontal line. The low and high fluence region, as referred to in this paper, are shown.

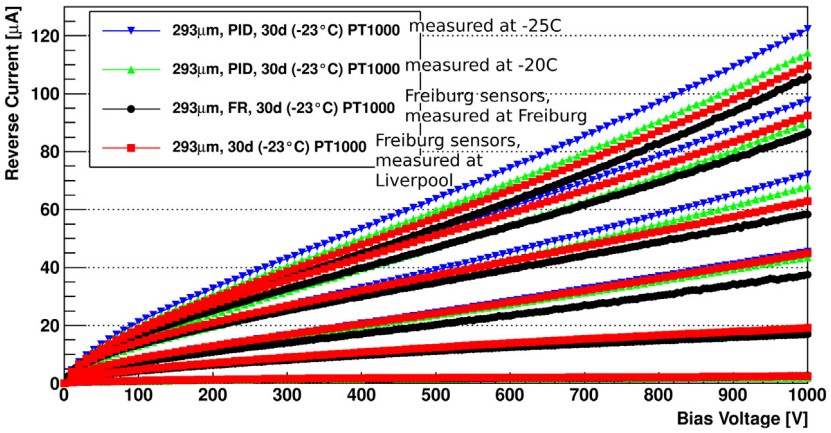

Fig. 6. Comparison of the reverse current for different irradiation fluences measured in Freiburg and Liverpool. The current measurements were scaled to a temperature of $T = -23\,^{\circ}\mathrm{C}$. The blue and green line show measurements with the same setup at different temperatures. The red and black lines show measurements at the setups in Liverpool and Freiburg, respectively. (For interpretation of the references to colour in this figure legend, the reader is referred to the web version of this article.)

Table 1
Literature values for α at 21 °C for the different annealing steps at room temperature, calculated for short term annealing and long term annealing. [6].

Annealing Time [d]	α [10^{-17} A/cm]	
	Short term	Long term
0.3	6.40 ± 0.43	6.24
10	4.32 ± 0.29	4.36
30	3.50 ± 0.23	3.61

Table 2
Averaged values for the effective energy for the three different annealing steps at room temperature.

Annealing time [d]	Effective energy [eV]
0.3	1.18 ± 0.03
10	1.20 ± 0.03
30	1.21 ± 0.03
Lit. value	1.214 ± 0.014

than the unknown depleted volume for highly irradiated devices. The calculated values of α^* are not constant with voltage since the actual depleted volume changes throughout the measurement. The literature values can be found in Table 1.

5. Results

5.1. Effective energy

In Fig. 4 the effective energy is displayed as a function of the applied bias voltage for one sensor. The averaged values of the effective energy for each sensor directly after irradiation and after 10 and 30 days annealing at room temperature are shown in Fig. 5, respectively. The averaged results of all sensors are also shown in Table 2. The values obtained for the effective energy agree within the uncertainties for the three different annealing times. The spread of the measured values for different sensors and different annealing times increases with higher irradiation fluence. Due to averaging of up to 200 measurements at different bias voltages the statistic uncertainty is reduced so that the already mentioned systematic uncertainty of 0.03 eV is solely dominating.

The effect of a decreasing effective energy to values below 1.0 eV for very high fluences ($> 1\times10^{16}\ \mathrm{n_{eq}/cm^2}$), which was observed in previous measurements [6], could be weakened by improving the cooling system of the measurement setup, as presented in this study. Still a slight deviation of results between measurements performed in Freiburg and Liverpool was observed. The magenta and green marker in Fig. 5(c) ('Liv. HPK') show the same set of sensors measured in Liverpool and in Freiburg. The different data analyses procedures proved to give the same results on the same dataset, so the observed deviation is resulting from the different experimental setup. This was confirmed by an exchange of the sensors, between Liverpool and Freiburg, which were used for the study. A detailed analysis of the different results was performed by Sven Wonsak [11].

There are several reasons that can lead to deviations in the measured values for the effective energy. For high fluences the increase of the reverse current is heating up the sensor and although the sensor temperature seems to be constant on the surface, a slightly higher 'real' sensor temperature would result in a reduced value for the effective energy. In addition, charge carriers from the non-depleted volume of the sensor can contribute to the reverse current at high bias voltages and irradiation fluence (active electrically neutral bulk, active ENB) [1]. In Fig. 6 one can see both the effect of different experimental setups and the uncertainty introduced by scaling measurements to different temperatures. The red and black line show measurements of the same sensors performed in Liverpool and Freiburg after 30 days of annealing at room temperature. The deviation of the measured values is more pronounced for higher irradiation fluences. The blue and green line show measurements performed at the same setup (Liverpool), but with a temperature difference of 5 °C. The measurement values were then scaled to $T = -23\,^{\circ}\mathrm{C}$ each. Also here the remaining deviation is higher for high irradiated devices.

5.2. Current related damage rate

In Fig. 7 the measured values for α^* can be seen for different sensors and irradiation fluences. Shown are measurements directly after irradiation and after 10 and 30 days annealing at room temperature, respectively. The thin Micron sensors reach values far above the literature value, which is displayed as a constant red line. This might be a result of a miss measured sensor volume, resulting in an overestimation of α^* (see Eq. (2)). Also charge multiplication or a beginning breakdown could lead to higher currents than expected. For the sensors, which were exposed to a lower irradiation fluence, especially for the Micron sensors, a kink in the voltage characteristic can be seen. Here it is likely that the full depletion voltage was reached. For higher irradiated sensors no clear transition from the non-depleted to depleted state is visible. The calculated values of α^* are smaller for higher irradiated sensors.

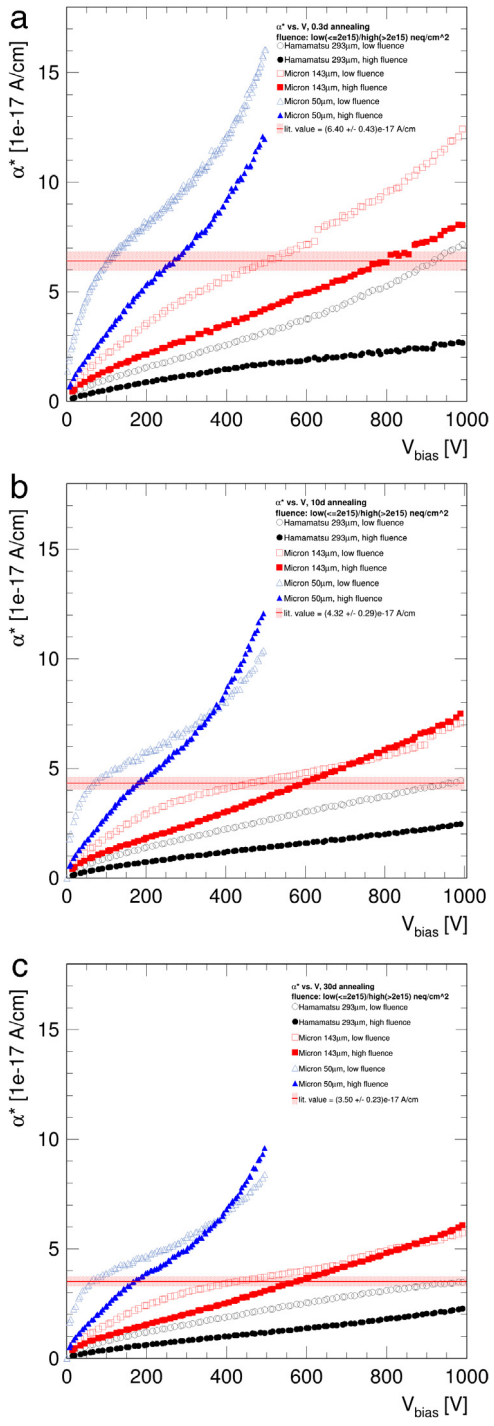

Fig. 7. Geometric current related damage rate α^* measured directly after irradiation (a) and after 10 (b) and 30 (c) days annealing at room temperature. The sensors are grouped into high ($>3\times10^{15}$ n_{eq}/cm^2) and low ($<3\times10^{15}$ n_{eq}/cm^2 irradiated devices. The literature value for the current related damage rate is indicated with a red line. (For interpretation of the references to colour in this figure legend, the reader is referred to the web version of this article.)

This is explained by the fact that for higher irradiated sensors the actual depleted volume is smaller, which is not accounted for in the calculation.

Furthermore one can see that the reduction of reverse current due to annealing of the sensor is more pronounced for less irradiated devices.

6. Conclusion

For this study the current–voltage characteristic of n-in-p mini silicon strip sensors was measured in order to calculate the effective energy and current related damage rate. The sensors were irradiated with fluences up to 2×10^{16} n_{eq}/cm^2 and measurements were performed directly after irradiation and after 10 and 30 days of annealing at room temperature. The aim was to determine if the parametrization models of the reverse current of silicon devices still hold for the high irradiation fluences expected at HL-LHC and future high energy physics experiments.

For low irradiation fluences the calculations of the effective energy are in good agreement with the expected value. For higher doses a tendency to lower values for the effective energy is visible, before and after annealing. As mentioned in Section 5.1 the picture of distinct depleted and non-depleted volumes of a silicon sensor does not hold for high irradiation fluences. Thus by construction the parametrization of the fluence dependence of the reverse current with a single parameter (α) has limited validity. For high irradiated devices at the highest bias voltages, the reverse current would have been underestimated by a factor of about 2.5 using the literature value of α for calculation (see Fig. 7). Thus a safety margin should always be applied. Furthermore the strong temperature dependence of the reverse current of irradiated devices poses limitations on the calculation of the effective energy. The precision of measurements depends more than for low irradiated sensors on the efficiency of the cooling system and the accuracy of the temperature measurement. If special care is taken to control these factors the parametrization models can be used to give an estimation of the expected reverse current in experiments even for high irradiation fluences.

This project has received funding from the European Union's Horizon 2020 Research and Innovation programme under Grant Agreement no. 654168.

References

[1] A. Chilingarov, Temperature dependence of the current generated in Si bulk, J. Instrum. 8 (10) (2013) P10003. URL http://stacks.iop.org/1748-0221/8/i=10/a=P10003.
[2] M. Moll, Radiation Damage in Silicon Particle Detectors (Ph.D thesis), Universität Hamburg, 1999.
[3] R. Wunstorf, Systematische Untersuchung zur Strahlenresistenz von Silizium-Detektoren für die Verwendung in Hochenergiephysik-Experimenten (Ph.D. thesis), Universität Hamburg, 1992.
[4] G. Lindstroem, M. Moll, E. Fretwurst, Radiation hardness of silicon detectors a challenge from high-energy physics, Nucl. Instrum. Methods Phys. Res. A 426 (1) (1999) 1–15. http://dx.doi.org/10.1016/S0168-9002(98)01462-4.
[5] M. Moll, E. Fretwurst, G. Lindstroem, Leakage current of hadron irradiated silicon detectors material dependence, Nucl. Instrum. Methods Phys. Res. A 426 (1) (1999) 87–93. http://dx.doi.org/10.1016/S0168-9002(98)01475-2.
[6] S. Wonsak, A. Affolder, G. Casse, P. Dervan, I. Tsurin, M. Wormald, Measurements of the reverse current of highly irradiated silicon sensors, Nucl. Instrum. Methods Phys. Res. A (2015).
[7] P.S. Miyagawa, I. Dawson, Radiation Background Studies for the Phase II Inner Tracker Upgrade. Tech. Rep. ATL-UPGRADE-PUB-2014-003, CERN, Geneva, 2014 URL https://cds.cern.ch/record/1753332.
[8] G. Kramberger, V. Cindro, M. Mikuž, M. Milovanović, M. Zavrtanik, et al., Investigation of irradiated silicon detectors by edge-tct, IEEE Trans. Nucl. Sci. 57 (4) (2010) 2294–2302.
[9] H.P.K.K., URL http://www.hamamatsu.com/, 2015.
[10] M.S. Ltd., URL http://www.micronsemiconductor.co.uk/, 2015.
[11] S. Wonsak, Characterisation of Irradiated Planar Silicon Strip Sensors for HL-LHC Applications (Ph.D. thesis), University of Liverpool, 2016.